Supplementary material for: “Analytical approximations to the flow field induced by electroosmosis during isotachophoretic transport through a channel“

By Tobias Baier, Friedhelm Schönfeld & Steffen Hardt

Journal of Fluid Mechanics, vol. XXX (201X), pp. XX-XX

Appendix A: The flow field for a stepwise change in EOF velocity (using Papkovich-Fadle functions)

To a certain extent the analysis presented here relates to analytical solutions for the EOF field in channels with an inhomogeneous zeta potential. In particular, Anderson and Idol [Anderson and Idol, 1985] studied the flow in a circular capillary with a periodically varying zeta potential in the axial direction, and Horiuchi et al. [Horiuchi et al., 2007] calculated the flow field for a step change in the zeta potential in a parallel-plates geometry. Similarly, Ajdari [Ajdari, 1995] and Stroock et al. [Strook et al., 2000] as well as Qian and Bau [Qian and Bau, 2002] investigated periodic variations of the zeta potential in parallel-plates geometries (c.f. Appendix B). Long et al. [Long et al., 1999] calculated the EOF for point defects in planar and cylindrical geometries as well as for ring defects in cylindrical geometries. Lubrication theory was used by Ghosal [Ghosal, 2002b] to calculate the EOF field for a slowly varying zeta potential along a channel. The related problem of planar electroosmotic flow near a surface charge discontinuity in a semi infinite fluid domain was studied by Yariv [Yariv, 2004].

Here we intend solving the biharmonic equation in a planar geometry with a step change in the EOF velocity using Papkovich-Fadle eigenfunctions. The boundary conditions for the problem are depicted in Figure 10. At the channel walls ($y = \pm 1$), the impermeability condition $u_y = 0$ determines the *x*-derivatives of the stream function; the *y*-derivatives are determined by the Helmholtz-Smoluchowski boundary condition of equations (13) and (2) in the main text. These boundary conditions are based on the assumption that the width of the ITP transition zone is much smaller than the channel width, i.e. a step-like transition at $x = 0$ is assumed. We will use the decomposition of the stream function into near-field and far-field solutions as specified in equation (14). Since the far-field solutions obey the velocity boundary conditions at the wall, sketched in Figure 10, the wall boundary conditions for the near field solution are

$$\partial_x \psi_\delta(x,y)|_{y=\pm 1} = 0, \quad \partial_y \psi_\delta(x,y)|_{y=\pm 1} = 0. \tag{27}$$

Moreover, far away from the interface the near-field solution has to vanish

$$\lim_{x\to\pm\infty} \psi_\delta(x,y) = 0. \tag{28}$$

Since the first wall boundary condition, equation (27), demands that ψ_δ is constant everywhere at the wall, we can choose $\psi_\delta(x,y)|_{y=\pm 1} = 0$ without loss of generality. The symmetry of the problem is such that the velocity field has a positive parity with respect to an inversion of the *y*-axis, translating to a negative parity of the corresponding stream function, i.e. $\psi(-y) = -\psi(y)$. From the negative parity of the far-field solutions it then follows that also the near-field solution is required to have negative parity.

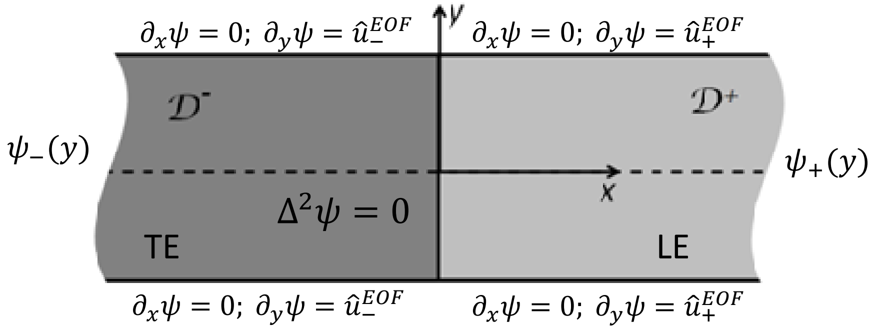

Figure 10 Illustration of the boundary conditions for the stream function $\psi(x, y)$. The wavy lines on both sides indicate that the corresponding boundary conditions are to be imposed at the two far ends of the channel. The coordinate system moves with the average EOF velocity relative to the laboratory system and the transition zone is located at x=0 at the particular time considered.

Solutions of the biharmonic equation (11) are sought in separable form

$$\psi_\delta \sim \Phi_1(y)e^{\lambda x}. \tag{29}$$

With the definition

$$\Phi_2(y) = \left(\partial_y^2 + \lambda^2\right)\Phi_1(y), \tag{30}$$

the biharmonic equation reduces to an eigenvalue problem

$$L\,U = \lambda^2 U, \tag{31}$$

where

$$U = \begin{pmatrix} \Phi_1 \\ \Phi_2 \end{pmatrix}, \qquad L = \begin{pmatrix} -\partial_y^2 & 1 \\ 0 & -\partial_y^2 \end{pmatrix}. \tag{32}$$

To simplify notation, we define the inner product between two such vectors $U = (\Phi_1, \Phi_2)^T$ and $V = (\psi_1, \psi_2)^T$as

$$\langle U|V\rangle = \int_{-1}^{1} dy\,\{\Phi_1(y)\psi_1(y) + \Phi_2(y)\psi_2(y)\}. \tag{33}$$

Following the analysis of [Kamke, 1962] and [Shankar, 2003] it is then straightforward to show that two eigenvectors U and V with eigenvalues λ and ν, i.e. $LU = \lambda^2 U$, $L^+V = \nu^2 V$, fulfil the biorthogonality relation, i.e.

$$\langle V|U\rangle = 0 \quad \text{for } \lambda \neq \nu, \tag{34}$$

where L^+ denotes the adjoint operator of L, defined by $\langle V|LU\rangle = \langle L^+V|U\rangle$.

We may further proceed as in [Shankar, 2003] to solve the biharmonic equation $\Delta^2\psi_\delta(x, y) = 0$ in the two semi-infinite domains $\mathcal{D}^-$ and $\mathcal{D}^+$shown in Figure 10 with the boundary conditions

$$\begin{aligned} &i)\ \ \psi_\delta(x, \pm 1) = \partial_y\psi_\delta(x, y)|_{y=\pm 1} = 0, \\ &ii)\ \lim_{|x|\to\infty} \psi_\delta(x, y) = 0, \\ &iii)\ \psi_\delta(0^\pm, y) = P_\pm(y), \end{aligned} \tag{35}$$

$$iv)\ \Delta\psi_\delta(x,y)|_{x=0^\pm} = \left(\partial_x^2 + \partial_y^2\right)\psi_\delta(x,y)|_{x=0^\pm} = Q_\pm(y),$$

where

$$\mathcal{D}^- = \{(x,y) \mid x \le 0 \wedge |y| < 1\} \quad \text{and} \quad \mathcal{D}^+ = \{(x,y) \mid x \ge 0 \wedge |y| < 1\}. \tag{36}$$

$P_\pm(y)$ and $Q_\pm(y)$ are functions that need to be determined from the requirements that at $x = 0$ the velocity field is continuous and the corresponding stream function solves the biharmonic equation. The notation $0^\pm$ symbolises taking the limit for positive and negative values of x, respectively. We extend Shankar's analysis to antisymmetric short edge boundary conditions, i.e. $P_\pm(-y) = -P_\pm(y)$ and $Q_\pm(-y) = -Q_\pm(y)$. In this case the eigenfunctions of equation (31) are given by the odd Papkovich-Fadle eigenfunctions [Smith, 1952; Joseph, 1977]

$$\begin{aligned}\hat{\varphi}_{1,\lambda}(y) &= \lambda\cos\lambda\sin\lambda y - \lambda y\sin\lambda\cos\lambda y\\ \hat{\varphi}_{2,\lambda}(y) &= 2\lambda^2\sin\lambda\sin\lambda y,\end{aligned} \tag{37}$$

which obey $L\,\hat{U}_\lambda = \lambda^2\hat{U}_\lambda$, where $\hat{U}_\lambda = \left(\hat{\varphi}_{1,\lambda}, \hat{\varphi}_{2,\lambda}\right)^T$. The complex eigenvalues are solutions of the equation

$$\sin 2\lambda = 2\lambda. \tag{38}$$

Note that if λ is an eigenvalue, so is its complex conjugate $\bar{\lambda}$ as well as $-\lambda$, so it suffices to tabulate values in the first quadrant of the complex plane. We will order these eigenvalues according to their ascending real parts as λ_n, $n \in \mathbb{N}_0$. The first eigenvalues are $\lambda_0 = 0$, $\lambda_1 = 3.74884 + 1.38434i$ and $\lambda_2 = 6.94998 + 1.6761i$. We extend this notation so that negative indices refer to the complex-conjugate values, i.e. $\lambda_{-n} = \bar{\lambda}_n$.

Since $L^+ = L^T$, we immediately get the corresponding eigenfunctions $\hat{V}_\nu$ with eigenvalue ν of the adjoint operator L^+ fulfilling $L^+\hat{V}_\nu = \nu^2\hat{V}_\nu$, $\hat{V}_\nu =: \left(\hat{\psi}_{1,\nu}, \hat{\psi}_{2,\nu}\right)^T = \left(\hat{\varphi}_{2,\nu}, \hat{\varphi}_{1,\nu}\right)^T$.

The boundary conditions (iii) and (iv) can now be expanded in terms of the eigenfunctions $\hat{U}_\lambda$ and the expansion coefficients a_λ can be determined by making use of equation (33):

$$\Pi_\pm(y) = \begin{pmatrix} P_\pm(y) \\ Q_\pm(y) \end{pmatrix} = \sum_\lambda a_\lambda^\pm \hat{U}_\lambda(y), \tag{39}$$

$$a_\lambda^\pm = \frac{\langle \hat{V}_\lambda | \Pi_\pm \rangle}{\langle \hat{V}_\lambda | \hat{U}_\lambda \rangle} = -\frac{\langle \hat{V}_\lambda | \Pi_\pm \rangle}{4\lambda^2 \sin^4\lambda}, \tag{40}$$

where the sum extends only over eigenvalues with positive (negative) real parts for solutions in $\mathcal{D}^-$ ($\mathcal{D}^+$).

The general form of the solution in the domains $\mathcal{D}^-$ and $\mathcal{D}^+$ fulfilling the boundary conditions of equation (35) is then given by

$$\psi_\delta^\pm(x,y) = \sum_\lambda a_\lambda^\pm\ \hat{\varphi}_{1,\lambda}(y)\, e^{-\lambda|x|}, \tag{41}$$

where the sum only extends over eigenvalues with strictly positive real part in order to meet boundary condition (ii). We will use this summing convention in the following without explicitly mentioning it.

For completeness and convergence properties of the biharmonic expansion (41) we refer the reader to [Gregory, 1980; Joseph et al., 1977, 1978, 1982; Spence, 1983]. For large x this expression is dominated by the first eigenvalue λ_1, so the near field solution drops off rapidly within the region spanning $\Delta x \sim -\ln 0.01/\mathrm{Re}\,\lambda_1 = 1.23$ at both sides of $x = 0$.

Application to the transition zone problem

We will now determine the expansion coefficients in equation (41) for the specific case of the flow field around a narrow isotachophoretic transition zone. The two domains $\mathcal{D}^-$ and $\mathcal{D}^+$ are coupled via the boundary conditions at $x = 0$, resulting in different expansion coefficients in the two domains. However, due to the fact that the *y*-velocity has to be continuous when crossing $x = 0$ we immediately see that the expansion coefficients in the biharmonic series must be equal in magnitude and of opposite sign in $\mathcal{D}^-$ and $\mathcal{D}^+$. The near field solution in $\mathcal{D}^- \cup \mathcal{D}^+$ can thus be written in the form

$$\psi_\delta(x,y) = \mathrm{sign}(-x) \sum_\lambda a_\lambda\, \hat{\varphi}_{1,\lambda}(y)\, e^{-\lambda|x|}, \tag{42}$$

where $\mathrm{sign}(x) = (2\Theta(x) - 1)$ is the sign function. The near field solution thus has a discontinuity at $x = 0$ whose magnitude is proportional to the difference in the far-field solutions. This simply reflects the fact that the full stream function has to be continuous at $x = 0$.

This leads us to the determination of the short edge boundary functions $P(y)$ and $Q(y)$. To obtain the first boundary condition we note that from the continuity of ψ at $x = 0$, it immediately follows that

$$P_-(y) = \psi_\delta(x = 0^-, y) = \tfrac{1}{2}\big(\psi_+(y) - \psi_-(y)\big) = \tfrac{1}{2}\alpha y(1 - y^2). \tag{43}$$

Since the biharmonic equation has to be fulfilled in the complete domain $\mathcal{D}^+ \cup \mathcal{D}^-$, we have to check that our ansatz equation (14) is also a valid solution at $x = 0$ and proceed by explicitely calculating each term in $\Delta^2\psi_\delta = \big(\partial_x^4 + 2\partial_x^2\partial_y^2 + \partial_y^4\big)\psi_\delta$. For the fourth derivative of ψ_δ with respect to x we write symbolically

$$\partial_x^4\psi_\delta(x,y) = \sum_\lambda a_\lambda \mathrm{sign}(-x)\, \hat{\varphi}_{1,\lambda}(y)\, \lambda^4\, e^{-\lambda|x|} + g(y)\partial_x^2\Theta(x), \tag{44}$$

where $g(y) = \sum_\lambda a_\lambda\, \hat{\varphi}_{1,\lambda}(y)\, \lambda^2 = \partial_x^2\psi_\delta(x,y)|_{x=0^\pm}$. The last notation denotes the right/left derivatives of the function $\psi_\delta(x,y)$ at $x = 0$. The other terms become

$$\begin{aligned} \partial_x^2\partial_y^2\psi_\delta(x,y) &= -\sum_\lambda a_\lambda \mathrm{sign}(-x)\, \hat{\varphi}_{1,\lambda}(y)\, \lambda^4\, e^{-\lambda|x|} \\ &\quad + 2\sum_\lambda a_\lambda \mathrm{sign}(-x) \sin\lambda \sin\lambda y\;\, \lambda^4\, e^{-\lambda|x|}, \\ \partial_y^4\psi_\delta(x,y) &= \sum_\lambda a_\lambda \mathrm{sign}(-x)\, \hat{\varphi}_{1,\lambda}(y)\, \lambda^4\, e^{-\lambda|x|} \\ &\quad - 4\sum_\lambda a_\lambda \mathrm{sign}(-x) \sin\lambda \sin\lambda y\;\, \lambda^4\, e^{-\lambda|x|}. \end{aligned} \tag{45}$$

Collecting terms, we see that the biharmonic equation is fulfilled everywhere only if $g(y) = 0$, i.e. $\partial_x^2\psi_\delta(x,y)|_{x=0^\pm} = 0$, since this eliminates the term with the ill-defined second derivative of the

Heaviside (step) function. This leads to the second of the short edge boundary conditions and we obtain

$$Q_{-}(y) = \left(\partial_x^2 + \partial_y^2\right)\psi_\delta(x,y)|_{x=0^-} = P_{-}''(y). \tag{46}$$

From equations (43) and (46) we obtain via equation (40)

$$a_\lambda = \frac{-4\alpha \sin^2 \lambda}{-4\lambda^2 \sin^4 \lambda} = \frac{\alpha}{\lambda^2 \sin^2 \lambda}. \tag{47}$$

Collecting terms, we have

$$\psi_\delta(x,y;\alpha) = -\alpha\ \mathrm{sign}(x) \sum_\lambda \frac{1}{\lambda^2 \sin^2(\lambda)} \hat{\varphi}_{1,\lambda}(y)\ \mathrm{e}^{-\lambda|x|}, \tag{48}$$

where the dependence on α has been made explicit in the notation for ψ_δ. The boundary conditions $\Pi(y)$ at $(x,y) = (0,\pm 1)$ are not consistent with the boundary conditions obeyed by the Papkovich-Fadle eigenfunctions themselves. In particular, $\partial_y \hat{\varphi}_{1,\lambda}(y)|_{y=\pm 1} = 0$, while $\partial_y P_{-}(y)|_{y=\pm 1} = -\alpha$. This suggests some discontinuous behaviour of the derivatives of the stream function at $(x,y) = (0,\pm 1)$, as already pointed out by Joseph [Joseph, 1982]. Further note that only these points are problematic for the convergence of the series, since for $|x| > 0$ the terms are strongly damped by the $e^{-\lambda|x|}$-factors, and the series will still give a faithful representation of the solution to the differential equation.

It is well known that Fourier series expansions suffer from “Gibbs ringing” in the vicinity of discontinuities. The same is expected for the expansion in biharmonic eigenfunctions and has already been pointed out by Joseph [Joseph et al., 1978, 1982]. In order to reduce this effect we replace the sums by their respective Cesaro sums, i.e. instead of summing a sequence $a_i, i \in \mathbb{N}$ we do a weighted summation over the respective partial sums $s_n = \sum_{i=1}^{n} a_i$. In particular, we replace the truncated sum $s_N = \sum_{i=1}^{N} a_i$ by $s_N^C = \frac{1}{N}\sum_{i=1}^{N} s_i = \sum_{i=1}^{N} \frac{(N-n+1)}{N} a_i$. We will refer to the truncated sums s_N as the “plain summation” and to s_N^C as the corresponding “Cesaro summation”.

In Figure 11 we explore both of the aspects mentioned in the previous paragraphs. As can be seen from the figure, the sums for $\psi_\delta(0^-,y)$ converge well, although it is apparent that the Cesaro summation yields a much smoother curve. By contrast, the sum for $\partial_y \psi_\delta(0^-,y)$ converges much slower, and due to the fact that the derivative of the odd biharmonic eigenfuctions vanishes at the boundary, always has a discontinuity at the wall. For the plain summation it even seems that the sum always lies within a band around the functional value. The width of this band does not seem to get reduced significantly below the value obtained with 50 terms even when summing a larger amount of terms. In the following, if not stated otherwise, the analysis is done by adding the first 250 terms of the Cesaro sum, where only eigenvalues λ in the first quadrant of the complex plane have to be considered, since the eigenvalues appear as complex-conjugate pairs (i.e. the fourth quadrant is included automatically when taking twice the real part of the sum over the first quadrant).

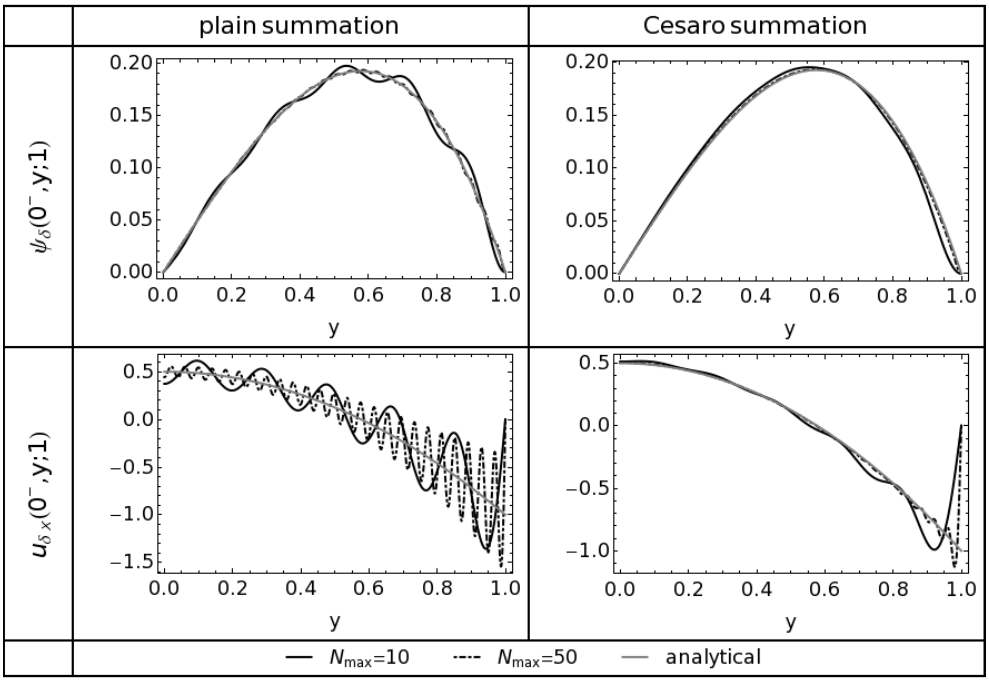

Figure 11 Convergence of the series expansions for $\psi_\delta(0^-,y;1)=\frac{1}{2}y(1-y^2)$ and $u_{\delta x}(0^-,y;1)=\partial_y\psi_\delta(0^-,y;1)$; Left: plain sum, Right: Cesaro sum. The sums run over N_{max} complex-conjugate pairs of eigenvalues in the first and fourth quadrant of the complex plane.

To summarize, in the frame of reference co-moving with the average EOF velocity, the stream function and the components of the velocity field are given by

$$\psi(x,y)=\alpha\left(-y[1-y^2]\{\Theta(-x)-l\}-\operatorname{sign}(x)\sum_n\frac{1}{\lambda_n^2\sin^2\lambda_n}\hat{\varphi}_{1,\lambda_n}(y)\,e^{-\lambda_n|x|}\right)$$

$$\hat{u}_x(x,y)=\alpha\left(-[1-3y^2]\{\Theta(-x)-l\}-\operatorname{sign}(x)\sum_n\frac{1}{\lambda_n^2\sin^2\lambda_n}\partial_y\hat{\varphi}_{1,\lambda_n}(y)\,e^{-\lambda_n|x|}\right) \tag{49}$$

$$\hat{u}_y(x,y)=\sum_n a_n\hat{\varphi}_{1,\lambda_n}(y)\,\lambda_n e^{-\lambda_n|x|}.$$

Note that the only independent parameters in these expressions are α and l. We remark that this form is equivalent to the one obtained by Horiuchi et.al. by Laplace transform methods [Horiuchi et.al., 2007].

Appendix B: Alternative representation for the flow field for a stepwise change in the EOF velocity (Meleshko's method of superposition)

An alternative representation for the flow field $\psi_\delta(x,y;\alpha)$ can be obtained by the superposition method for the biharmonic equation developed for the problem of steady Stokes flow in a rectangular cavity by Meleshko [Meleshko, 1996]. We will use the solution of Qian and Bau [Qian and Bau, 2002] for the biharmonic equation in a cavity defined by the region $(x,y)\in[-h,h]\times[-1,1]$, using dimensionless coordinates. The velocity $u_x(x,y)|_{y=\pm1}=\operatorname{sign}(x)$ is prescribed at the top and bottom surfaces and the shear rate $\partial_x u_y(x,y)|_{x=\pm h}=0$ at the side walls. Their solution reads

$$\psi^{MQB}(x,y) = -\frac{4}{h}\left(\sum_{\substack{m=1\\ m\ odd}}^{\infty} \frac{(-1)^m}{\alpha_m} q_m p_m(y)\, sin(\alpha_m x) - \sum_{\nu=0}^{\infty}\big(S(x, 2\nu+1-y) - S(x, 2\nu+1+y)\big)\right), \tag{50}$$

where $\alpha_m = \frac{m\pi}{h}$, and we have used the abbreviations

$$p_m(y) = \coth\alpha_m \frac{\sinh\alpha_m y}{\sinh\alpha_m} - y\frac{\cosh\alpha_m y}{\sinh\alpha_m},\quad q_m = \left(\left(\frac{\alpha_m}{\sinh^2\alpha_m} - \coth\alpha_m\right)^{-1} + 1\right),$$
$$S(\xi,\eta) = -\frac{yh}{2\pi}\arctan\left(\frac{\sin\left(\frac{\pi x}{h}\right)}{\sinh\left(\frac{\pi y}{h}\right)}\right). \tag{51}$$

An approximation for $\psi_\delta(x,y;\alpha)$ may now be obtained for sufficiently large $h \gg 1$ and $|x| < \frac{h}{2}$ from

$$\psi_\delta(x,y;\alpha) = \alpha\left(\text{sign}(x)\ \frac{1}{2}y(1-y^2) - \psi^{MQB}(x,y)\right). \tag{52}$$

Truncating the x-domain from $x \in [-h, h]$ to $x \in [h/2, h/2]$ serves the purpose of attenuating the influence of the shear-stress boundary condition at $|x| = h$, which is inadequate in the present context. As an example, setting $h = 5$, and summing the first 10 terms in both sums gives an excellent approximation in the range $x \in [-2.5, 2.5]$. Since $\psi_\delta(x,y;\alpha)|_{x=\pm\frac{h}{2}}$ has already decreased by 5 orders of magnitude compared to its value at $x = 0$, which is more than sufficient for all practical purposes. Note that this representation has better convergence properties than the one presented in Appendix A and is in particular not plagued by the slow convergence at $x = 0$, since the sums in $\psi^{MQB}(x,y)$ yield a smooth function.

Appendix C: Electroneutrality and the influence of Maxwell stresses on the velocity field around an ITP transition zone

Maxwell stresses become increasingly important once the transition zone becomes sufficiently narrow and the electric fields large. With the charge density given by Gauss' law as

$$\rho = \nabla\cdot(\varepsilon\mathbf{E}), \tag{53}$$

where ε is the permittivity of the medium, the Stokes equation including the Maxwell stresses becomes

$$0 = \eta\Delta\mathbf{u} - \nabla p + \rho\mathbf{E}. \tag{54}$$

The electric and species concentration fields can be calculated as described for the NPS model. At first glance it may seem contradictory to on the one hand impose electroneutrality, i.e. $\sum_i z_i c_i = 0$, for determining the concentration as well as the electric fields and on the other hand use Gauss' law (53) for determining the charge density for the momentum equation, since on a fundamental level $\rho = F\sum_i z_i c_i$. However, it is important to note that compared to the concentrations of the ions, which is typically of the order of $c_0 \sim 10^{-2}$ mol/l, the induced charge density can safely be neglected in the Nernst-Planck equation [Newman and Thomas-Alyea, 2004]. We can estimate the induced charge density $\rho \sim \varepsilon E_0/\delta$ from a typical width δ~10 µm of the transition zone and the scale of the electric field $E_0 \sim 1$ kV/cm. Using a relative electric permittivity of ε_r~80, the ratio κ between the concentration of charge carriers and the bulk concentration is of the order

$$\kappa = \frac{\rho/F}{c_0} \sim \mathcal{O}(10^{-5}). \tag{55}$$

Due to the smallness of this parameter the deviation from electroneutrality may thus safely be neglected in the Nernst-Planck equations. In the spirit of a perturbation approach, expanding concentration and electric fields in κ, the equations of $\mathcal{O}(\kappa^0)$ are just the Nernst-Planck equations obeying the electroneutrality assumption as employed in this study, while Gauss' law connects the electric field obtained in $\mathcal{O}(\kappa^0)$ with the concentration fields of $\mathcal{O}(\kappa^1)$.

In order to assess the importance of the Maxwell stresses in the context of the present approximation we have included this term in the NPS model described in the main text and calculated the stream function as well as concentration fields for different current densities, c.f. Figure 12. In order to be able to directly compare with the original model, these results have been overlaid to plots of the respective results obtained in the NPS model without the Maxwell stresses. Since the electric field gradients in the transition zone increase for larger applied current densities and consequently the charge density increases, we have chosen three different current densities ranging from 0.4 kA/m² to 1.0 kA/m². As can be seen, the inclusion of Maxwell stresses does have some impact on the stream function for large applied current densities. Nevertheless, at least in the range considered the corresponding change in the velocity field only has a small impact on the concentration field at the transition zone. This indicates that Maxwell stresses play a minor role in typical ITP experiments. Nevertheless, at even larger applied fields the Maxwell stresses may dominate the flow and ion transport at a transition zone and even lead to instabilities. For example, a deformation of transition zones may occur even in the case of vanishing electroosmotic flow. However, the analysis of this effect lies outside the scope of the present study.

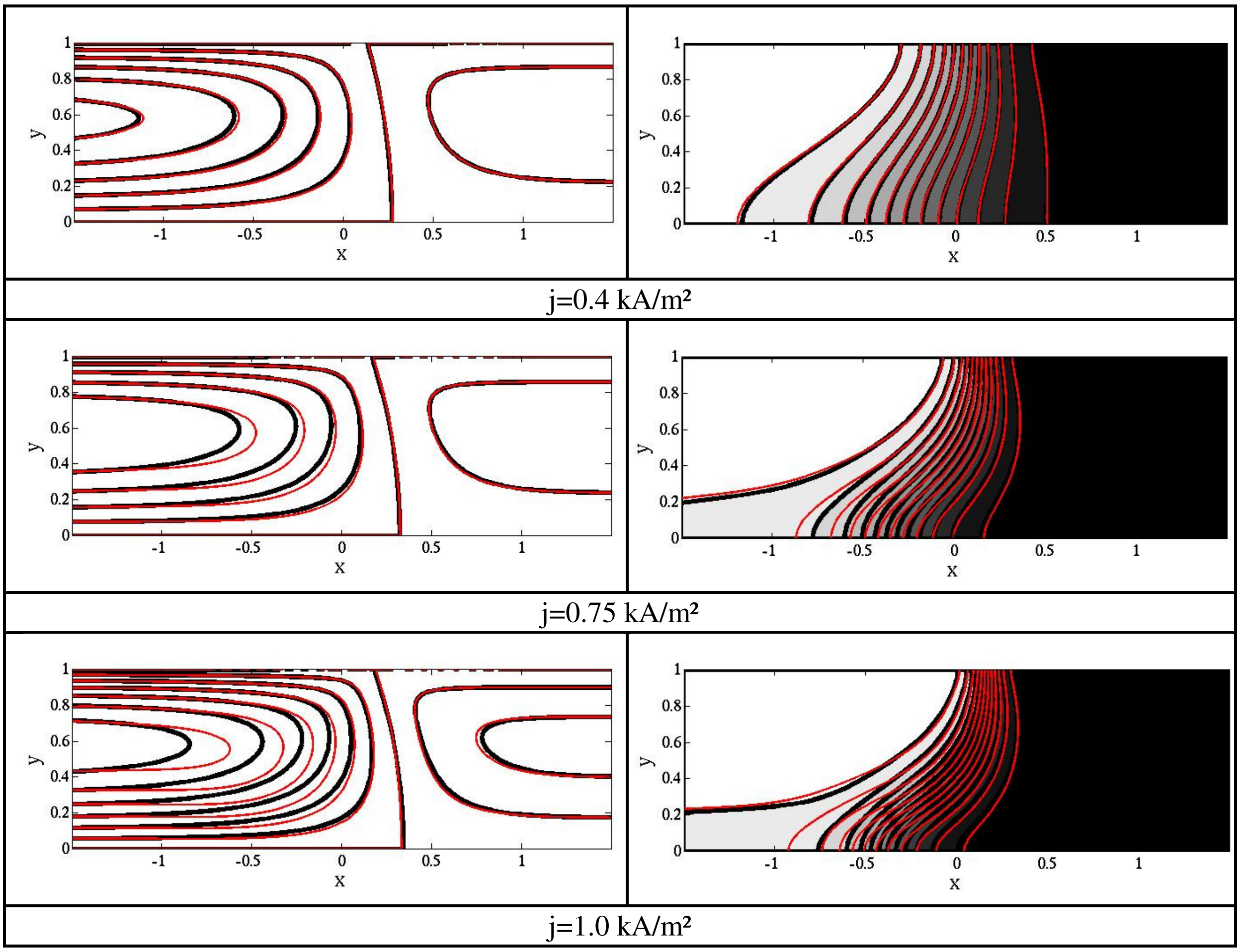

Figure 12 Left column: Contour lines of the normalised stream function as calculated in the NPS model without (black) and with Maxwell stresses (red) with (from top to bottom) $j = 0.4,\ 0.75,\ 1.0\ \mathrm{kA/m^2}$. All other parameters were chosen according to equation (25). Right column: TE ion concentration profiles as calculated in the NPS model without (greyscale) and including Maxwell stresses (red). Light and dark shades correspond to high and low concentrations of TE ions, respectively.

REFERENCES

AJDARI, A. 1996 "Generation of transverse fluid currents and forces by an electric field: Electro-osmosis on charge-modulated and undulated surfaces", *Phys.Rev.* **E 53**, 5, 4996-5005.

ANDERSON, J.W. & IDOL, W.K. 1985 "Electroosmosis trough pores with nonuniformly charged walls", *Chem.Eng.Comm.* **38**, 3, 93-106.

GHOSAL, S. 2002b "Lubrication theory for electro-osmotic flow in a microfluidic channel of slowly varying cross-section and wall charge", *J. Fluid Mech.* **459**, 103-128.

GREGORY, R. D. 1980 "The semi-infinite strip $x \geq 0$, $-1 \leq y \leq 1$; completeness of the Papkovich-Fadle eigenfunctions when $\Phi_{xx}(0,y)$ & $\Phi_{yy}(0,y)$ are prescribed", *J. Elasticity* **10**, 57-80.

HORIUCHI, K., DUTTA, P. & IVORY C. F. 2007 "Electroosmosis with Step Changes in Zeta Potential in Microchannel Electrophoresis," *AIChE J.* **53**, (10), 2521-2533.

JOSEPH, D. D. 1977 "The convergence of biorthogonal series for biharmonic and Stokes flow edge problems, Part I", *SIAM J. Appl. Math.* **33**, 337-347.

JOSEPH, D. D. & STURGES, L. 1978 “The convergence of biorthogonal series for biharmonic and Stokes flow edge problems, Part II”, *SIAM J. Appl. Math.* **34**, 1, 7-26.

JOSEPH, D. D., STURGES, L. & WARNER, W. H. 1982 “Convergence of biorthogonal series of biharmonic eigenfunctions by the method of Titchmarsh”, *Archive for Rational Mechanics and Analysis* **78**, 223 -274.

KAMKE, E. 1962 “Differentialgleichungen“, *Akad.Verlagsgesellschaft*, Leipzig.

LONG, D., STONE, H.A. & AJDARI, A. 1999 “Electroosmotic flows created by surface defects in capillary electrophoresis”, *Journal of Colloid and Interface Science* **212**, 338–349.

MELESHKO, V.V. 1996 “Steady Stokes flow in a rectangular cavity”, *Proc.R.Soc.Lond.* A **452,** 1999-2022.

NEWMAN, J. S. & THOMAS-ALYEA, K. E. 2004 “Electrochemical systems”, 3rd ed., Wiley, Hoboken (NJ).

QIAN S. & BAU H.H. 2002 “A chaotic electroosmotic stirrer”, *Analytical Chemistry*, **74**, 3616-3625.

SHANKAR P.N. 2003 “On the use of biorthogonality relations in the solution of some boundary value problems for the biharmonic equation”, *Curr. Sci.* **85**, 7, 975-979.

SMITH, R. T. C. 1952 “The bending of a semi-infinite strip”, *Austral. J. Sci. Res. A* **5,** 227-237.

SPENCE, D.A. 1983 “A class of biharmonic end-strip problems arising in elasticity and Stokes flow”, *IMA J. Appl.Math.*, **30**, 107–139.

STROOCK, A.D., WECK, M., CHIU, D.T., HUCK, W.T.S., KENIS, P.J.A., ISMAGILOV, R.F. & WHITESIDES, G.M. 2000 “Patterning Electro-osmotic Flow with Patterned Surface Charge”, *Phys.Rev.Lett.* **84**, 15, 3314-3317.

YARIV, E. 2004 “Electro-osmotic flow near a surface charge discontinuity”, *J. Fluid Mech.* **521**, 181-189.